

Modeling of pattern development during fibronectin nanofibril formation

Tilo Pompe^{a)}

Max Bergmann Center of Biomaterials Dresden, Leibniz Institute of Polymer Research Dresden, Hohe Straße 6, 01069, Dresden, Germany

Jörn Starruß

Center for Information Services and High Performance Computing, Technische Universität Dresden, 01062, Dresden, Germany

Manfred Bobeth

Institut für Werkstoffwissenschaft, Technische Universität Dresden, 01062, Dresden, Germany

Wolfgang Pompe

Max Bergmann Center of Biomaterials Dresden, Institut für Werkstoffwissenschaft, Technische Universität Dresden, 01062, Dresden, Germany

(Received 7 June 2006; accepted 26 July 2006; published 14 September 2006)

Formation of fibrillar fibronectin networks is a major process during embryogenesis and tissue formation, but the molecular details of fibril assembly remain poorly understood. Based on current ideas of fibronectin fibrillogenesis, a stochastic model was developed to enlighten the mechanism of the formation of paired fibronectin nanofibrils by adherent endothelial cells, which has been observed recently. The development of fibronectin clusters and fibrils was investigated by means of Monte Carlo simulations, including diffusion-controlled aggregation and myosin-driven transport of fibronectin-integrin complexes in the vicinity of a focal adhesion. Different evolving growth patterns were summarized in a morphological diagram as a function of the fibronectin substrate and fibronectin-fibronectin interaction energies. The formation of paired nanofibrils was found to occur in a certain region of interaction parameters. Beyond this region branched fibronectin clusters as well as tear-off of fibronectin fibrils were observed. © 2006 American Vacuum Society.

[DOI: 10.1116/1.2345653]

I. INTRODUCTION

Many adherent mammalian cells are able to assemble proteins in the extracellular space into a highly ordered fibrillar network. This network provides, e.g., intercellular mechanical stability and functional proximity of different cell types as basic prerequisites of tissue generation.¹ A major component of the extracellular matrix is fibronectin (FN)—a large glycoprotein (MW=440 000). The aggregation of FN molecules into fibrils has been intensively investigated in *in vitro* experiments with adherent cells on artificial substrates. The current understanding of fibril formation can be summarized as follows²⁻⁵ (see also Fig. 1):

- When cells adhere to a substrate surface via FN ligands, the transmembrane integrin receptors bind to the FN molecules. By this step, the integrins are activated, i.e., their intracellular and extracellular binding affinity increases due to conformational changes.
- Activated integrins bind to components of the cytoskeleton and start to form clusters within the cell membrane. Intracellular signaling leads to binding of further proteins and activation of downstream signaling cascades at those clusters. In this process, the integrins together with other proteins act as force-sensitive elements. They govern the signal transduction of applied

forces into biochemical reactions. Above a certain size of these clusters, they are called focal adhesions.

- FN fibril assembly is thought to occur at focal adhesions. The FN molecules at a focal adhesion are stretched and translocated via integrins from the primary adhesion site by a myosin-driven process along actin stress fibers (cf. Fig. 1). With participation of different kinds of integrins this process leads to fibril growth and formation of so-called fibrillar adhesions.^{2,3}
- FN fibril formation has been suggested to be triggered by exposing cryptic binding sites during stretch of FN molecules. The strong bond between FN molecules in the fibrils occurs via those cryptic sites.^{4,5}

Despite the wealth of details known about FN fibrillogenesis, the exact molecular assembly mechanism how cells form fibrils is poorly understood. To get further insight into this mechanism, a model experiment has recently been conducted to investigate how substrate-bound FN molecules are reorganized by the cells for different FN adsorption strengths on the substrate.^{6,7} In this experiment, endothelial cells were grown on polymer surfaces covered by FN molecules. The FN adsorption strength was varied by using different maleic anhydride copolymer surfaces as measured by protein heteroexchange experiments.⁸ During 50 min growth of cells on the FN covered substrates, they reorganize the FN molecules into a distinct fibrillar pattern. The experiment was performed for a short time to avoid secretion of FN from the cell. Besides the substrate-dependent micrometer scale pat-

^{a)}Author to whom correspondence should be addressed; electronic mail: pompe-tilo@ipfdd.de

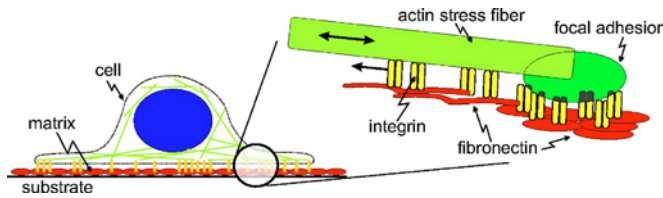


FIG. 1. Schematic of FN fibrillogenesis at focal adhesions.

tern, a scanning force microscopy (SFM) analysis revealed an additional nanometer scale pattern with paired nanofibrils as a peculiar feature after an extracellular cross-linking and removal of the cells⁷ (Fig. 2). The spacing between the two fibrils within paired nanofibrils increased with increasing FN adsorption strength. The observed discrete spacing values between these fibrils ranged from 70 to 400 nm, with their spacing found to occur as multiples of an average repeating unit of 71 nm. This repeating unit was proposed to be related to the special structure of the actin stress fibers. The reason for the appearance of the observed paired nanofibrils has not been explained yet.

Concerning the adhesion complexes of adherent cells, several theoretical investigations were recently performed to get further insight into the process of adhesion formation and its dependence on external and internal forces. Those studies were mainly focused on the growth, stability, and force sensitivity of focal adhesions. For example, the force regulation of early adhesions in dependence on the substrate rigidity has been described by a two state model of dynamical adhesion sites in Ref. 9. In another work, the dynamics of mature focal adhesions has been modeled by taking into account the elastic properties of mechanosensitive protein aggregates inside those complexes.¹⁰ The influences of the elastic properties of the proteins inside focal adhesions as well as of the characteristics of the extracellular matrix (i.e., elasticity, receptor binding) on the focal adhesions development were investigated in Refs. 11 and 12. This approach allowed to describe different experimentally observed growth regimes of focal adhesions like focal adhesion assembly and dissociation.

In this present study we concentrate on the development of fibrillar adhesions—mainly associated with FN fibrils—

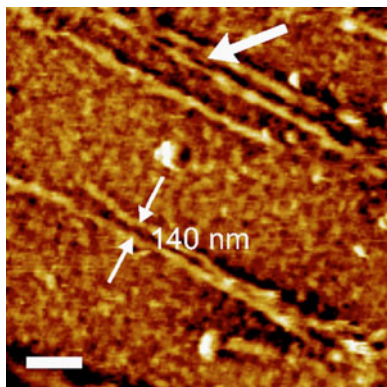


FIG. 2. SFM phase image of paired FN nanofibrils (arrows) investigated in Ref. 7. The spacing of paired nanofibrils is marked by arrows. Scale bar: 500 nm.

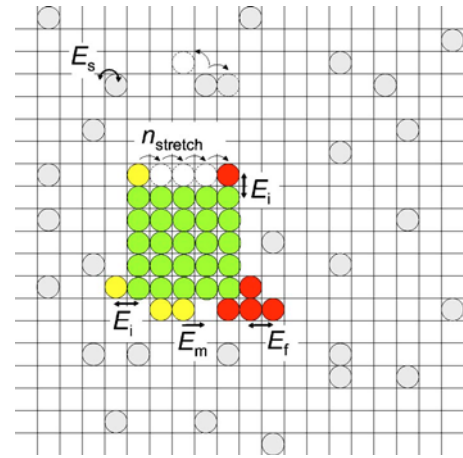


FIG. 3. Setup of the MC simulation. Complex types (light gray- C_{free} , yellow- C_{bound} , red- C_{stretch} , green- C_{fix}), jump directions, involved interaction energies as well as the stretching of FN molecules are shown.

out of an existing stationary focal adhesion as described above in the current understanding of FN fibril formation. Monte Carlo (MC) simulations were conducted as an attempt to help elucidate the molecular formation mechanism of paired fibrils and to estimate the interaction energies involved.

II. MATERIALS AND METHODS

A. Model description

On the basis of a model of integrin clustering on surfaces with FN ligands¹³ we developed the following MC simulation (cf. Fig. 3). The objects of the simulation are FN-integrin complexes C . Four types of complexes are distinguished: freely diffusing complexes C_{free} , fixed complexes resembling a focal adhesion C_{fix} , complexes weakly bound to the focal adhesion via intracellular bonds of the integrins C_{bound} , and complexes with stretched FN molecules C_{stretch} . Although the objects of the simulation are macromolecules, the migration of integrins within the cell membrane and the coupled FN molecules on the substrate (cf. Fig. 1) is modeled in a simple manner by a random walk of FN-integrin complexes on a two-dimensional (2D) square lattice of size $N \times N$. The complexes move by thermally activated jumps to unoccupied nearest and next nearest neighbor sites. The simulation starts at a stage where one focal adhesion has already been formed. The focal adhesion is approximated by a square-shaped cluster of fixed complexes C_{fix} of size $N_{\text{fix}} \times N_{\text{fix}}$. On the remaining lattice sites, N_{free} free complexes are distributed randomly.

The MC algorithm consists of the following loop. A complex and a jump direction are randomly chosen. If the corresponding neighboring site is free, the jump is performed with probability $p(E) = \exp(-E/kT)$ for $E > 0$ and $p(E) = 1$ for $E \leq 0$, where E is the energy associated with the designated jump. Then, the next complex is chosen.

The energy E is approximated by $E = E_s + E_{b,1} - E_{b,2} - E_m \Theta$. E_s is the activation energy for a jump, which corresponds to a substrate binding energy of a complex. $E_{b,1}$ and

$E_{b,2}$ are the binding energies to neighboring complexes before and after the jump, respectively ($E_{b,1}, E_{b,2} > 0$). The energy $E_{b,2}$ accounts for a lowering of the activation barrier for the binding of complexes to the cluster due to an attractive short-range interaction. This interaction is thought to result from the presence of additional proteins which are involved in the aggregation process at focal and fibrillar adhesions (e.g., vinculin, talin).²

The binding energy $E_b = n_i E_i + n_f E_f$ is obtained by counting the bonds to nearest and next nearest neighbors. The interaction energy E_i has been assigned to the $C_{\text{bound}} - C_{\text{fix}}$ and $C_{\text{stretch}} - C_{\text{fix}}$ bonds. It resembles the weak intracellular integrin-integrin interaction at the focal adhesion. The energy E_f for the $C_{\text{stretch}} - C_{\text{stretch}}$ bonds accounts for the strong FN-FN interaction of stretched FN molecules; n_i and n_f are the numbers of the corresponding bonds. The myosin-driven translocation of complexes along actin stress fibers away from the focal adhesion is roughly described by a lowering of the energy associated with a jump E by E_m . This applies in our model only to complexes C_{bound} and C_{stretch} for jumps in rightward direction, which has been chosen as the orientation of the actin stress fiber. In this case $\Theta = 1$ in the above formula for the energy E , and otherwise zero. By this mechanism a vectorial process is included to account for the directed myosin transport along the actin stress fibers.

The transition of the type C_{bound} to the stretched state C_{stretch} is accomplished by n_{stretch} consecutive thermally activated jumps along the boundary of the focal adhesion or growing fibril. This procedure simulates roughly the stretching of FN molecules in order to expose cryptic binding sites for the FN-FN assembly. Thus, by the transition of the complex from the bound to the stretched state, a favorable energy contribution is provided for the nucleation of fibrils at the focal adhesion and the growth of them towards the right side of the simulation cell. In our model, this process is driven by the parameter E_m in order to simulate the myosin-driven transport along the actin filament. When a stretched complex C_{stretch} leaves the fibril cluster, FN is supposed to back fold. Thus, the complex C_{stretch} transforms back to a free complex C_{free} .

B. Parameter set

The parameter values for the proposed simulation were chosen as follows. The effect of the actin stress fibers acting on the complexes was estimated by an energy E_m of 10 kT with T as room temperature. This estimate of the work done by myosin molecules moving along the stress fibers results from the measured force and step size of a single myosin molecule of 3–4 pN and 11 nm, respectively.^{14,15} The strong interaction between stretched FN molecules E_f was chosen comparable to other strong protein-protein interactions like receptor-ligand bonds of integrins (e.g., 20 kT for the $\alpha_5\beta_1$ -integrin-FN bond¹⁶). Correspondingly, values from 6 to 16 kT were used for E_f . The interaction energy between integrins in the integrin clusters is expected to be much smaller. Thus, the energy E_i was varied from 1 to 3 kT. The activation energy for jumps of free complexes E_s on the sub-

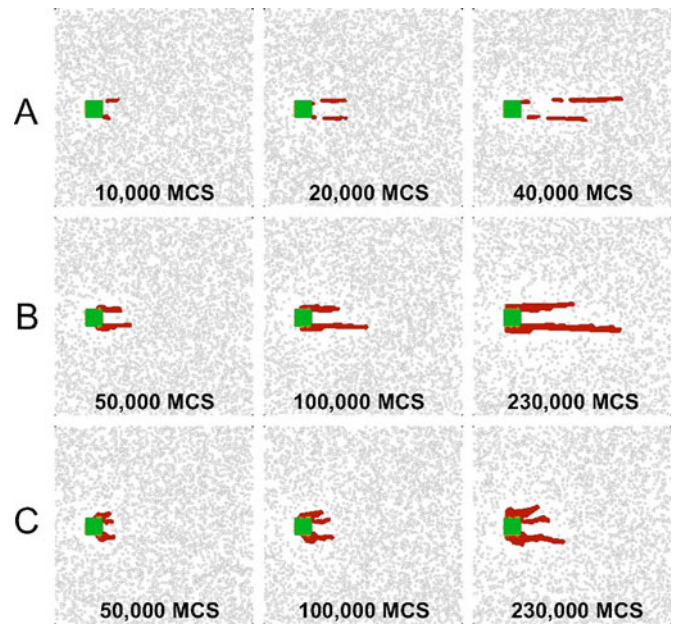


FIG. 4. Snapshots of pattern formation during MC simulation for typical examples of the three different growth regimes for a constant energy $E_s = 3$ kT: A-tear off of clusters ($E_f = 7$ kT), B-paired fibrils ($E_f = 10$ kT), C-branched pattern ($E_f = 13$ kT). The different types of complexes are indicated by different colors (light gray- C_{free} , yellow- C_{bound} , red- C_{stretch} , green- C_{fix}). The time of the snapshots is given in MCS.

strate was chosen in a range from 0.3 to 10 kT. This wide range accounts for the varying FN adsorption strengths on different substrates used in recent experiments.^{6,8}

Simulations were performed with a lattice size of $N = 256$. The lattice constant a_l was chosen equal to the size corresponding to one FN molecule for a substrate coverage of 250 ng/cm^2 .⁸ This results in a total length of the simulation cell of $4.3 \mu\text{m}$. The number of consecutive jumps, which are necessary to stretch a FN molecule, was estimated as $n_{\text{stretch}} = 4$ because cell-bound FN fibrils were found to shrink in size to one fourth when detached from the cells.¹⁷ This is supported by the finding that relevant FN domains (FN III) can be stretched by SFM 7–10 times of their original length. However, a fourfold stretching could be sufficient since cryptic binding sites are exposed already at partial stretch.⁴

At the beginning of the simulation, a focal adhesion is set with a fixed size of $N_{\text{fix}} = 9$ or $N_{\text{fix}} = 21$. These constant sizes are suggested by experimental findings in Refs. 6 and 7. On the remaining lattice sites, N_{free} free complexes were randomly distributed with a density corresponding to a typical integrin density in the cell membrane of $200 \mu\text{m}^{-2}$.¹⁸ The simulation time has been measured in terms of Monte Carlo steps (MCS), where one step is defined as N_{free} trials of moving a randomly chosen complex in a random direction. The duration of the simulation was adjusted in dependence on the evolving pattern. In the case of a characteristic growth of paired fibrils (i.e., $E_s = 3$ kT and $E_f = 10$ kT, cf. Fig. 4) the simulations were finished when the length of grown fibrils was comparable to experimental values of about $2 \mu\text{m}$.⁷ For

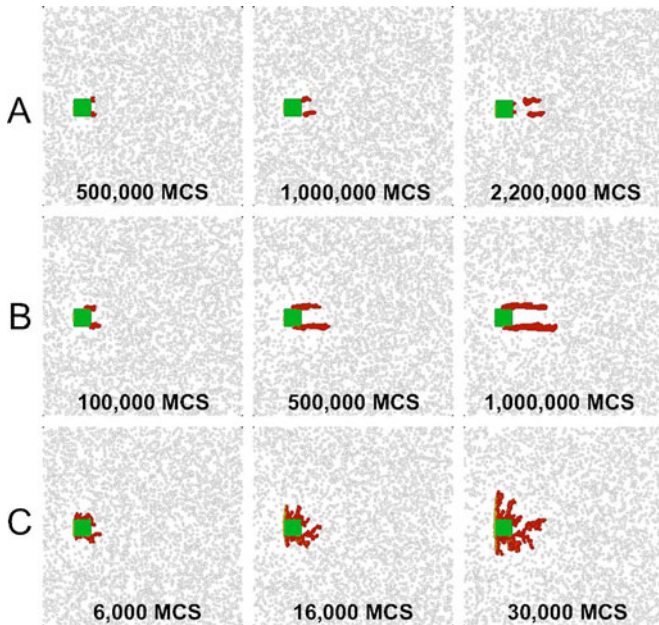


FIG. 5. Snapshots of pattern formation during MC simulation for typical examples of the three different growth regimes for a constant energy $E_f = 12$ kT: A-tear-off of clusters ($E_s = 7$ kT), B-paired fibrils ($E_s = 5$ kT), C-branched pattern ($E_s = 1$ kT). The time of the snapshots is given in MCS (coloring as in Fig. 4).

other parameter sets with lower or higher jump activation energy E_s , the simulations were performed until characteristic patterns had been evolved.

III. RESULTS AND DISCUSSION

Numerous MC simulations with 52 parameter sets for E_s and E_f and at least two repetitions for each set have been performed. Depending on the chosen parameter set, different patterns are observed for the aggregating clusters of integrin-FN complexes: branched patterns, tear-off fragments of fibrils, or paired fibrils. Snapshots at different simulation times in Figs. 4 and 5 illustrate the temporal evolution of characteristic patterns. The dependence of the patterns on the parameters E_s and E_f is exemplarily demonstrated by the variation of E_f in Fig. 4 and of E_s in Fig. 5. The growth patterns corresponding to the whole range of variations of the energy parameters E_s and E_f are summarized in a morphological diagram in Fig. 6 with $E_f = 1$ kT. In the diagram, three different growth regimes can be distinguished.

A regime with comparatively short and branched fibrils is found for small E_s and large E_f [see Fig. 4(C) and 5(C)]. Under the condition of relatively fast diffusion of the free complexes (small E_s), such a pattern results from the high value of FN-FN interaction E_f compared to the work E_m done by myosin molecules during integrin translocation. On the other hand, for low mobility of the free complexes (large E_s), the growth of fibrils at the focal adhesion is slow compared to the myosin-driven transport of complexes along the fibrils. As a consequence, the fibrils tend to tear off, as illustrated in Figs. 4(A) and 5(A). The separated FN clusters move rightwards by slip of the stretched complexes C_{stretch}

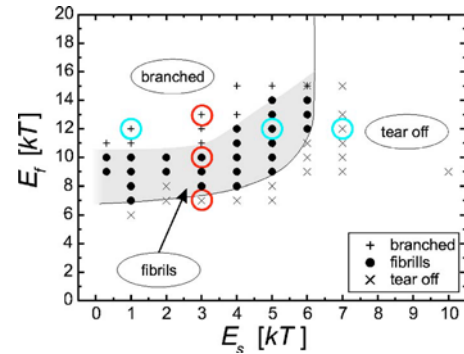


FIG. 6. Morphological diagram indicating three distinct growth regimes: a stress-controlled regime “tear-off,” a regime controlled by the strong FN-FN interaction “branched,” and a regime of paired fibril formation ($E_f = 1$ kT, $E_m = 10$ kT). Red and blue circles indicate typical examples of the different growth regimes, which are shown in detail in Figs. 4 and 5, respectively.

on the outside of the clusters. Tear-off of fibrils is also found for rather small values of E_f independent of E_s . The evolving pattern is comparable to experimental observations of transport of short fibril segments along actin stress fibers.³ The reason for the tear-off of small fibril segments is the limited supply of FN molecules towards the focal adhesion. In our model, this is caused by the slow diffusion of free complexes towards the fixed cluster. In the experiment the supply of FN molecules is artificially interrupted directly by changing the fluorescent-labeled FN in the cell culture medium.

The most striking feature is the growth of parallel oriented paired fibrils away from the focal adhesion as shown in Figs. 4(B) and 5(B). Typically, the growth of paired fibrils is found in the range from $E_s = 0.3$ –6 kT and $E_f = 8$ –13 kT with $E_f = 1$ kT (cf. black dots in Fig. 6). The spacing between the two parallel nanofibrils is determined by the size of the focal adhesion at the beginning of the simulation, which was verified by using different sizes of fixed clusters, see Sec. II. The peculiar fibril pattern results from the special growth mechanism: At first small FN fibrillar clusters nucleate. Later the clusters at the upper and lower side of the focal adhesion elongate due to myosin-driven transport in rightward direction. The latter process is simulated in the model by the energy parameter E_m , making jumps of C_{bound} and C_{stretch} to the right more favorable than to the left. In our 2D model, the two parallel elongated clusters hinder the diffusion of complexes into the region between them. Thus, assembly of further FN fibrils in this region is not possible. The paired nanofibril pattern obtained in the simulation is remarkably similar to the pattern observed in SFM investigations (cf. Fig. 2 and Ref. 7).

The conditions for paired fibril formation in the simulation have been compared with experimental findings.⁷ Patterns similar to the experimental observation in Fig. 2 were found for FN-substrate interaction energies $E_s = 1$ –6 kT. These values are compatible with estimates of differences between FN adsorption energies on different polymer substrates of 0.5–2 kT. The energy differences were derived from protein adsorption and protein heteroexchange experiments, as well as from cell culture studies.^{6,19} Furthermore,

the diffusion coefficient of free complexes in the simulation can be compared with known values of the diffusion coefficient of integrins within cell membranes. From the mean square displacement of a particle diffusing in two dimensions, the diffusion coefficient in the present context is estimated by $D = a_l^2 / 4\tau$, where τ is the mean waiting time between two jumps of a free complex and a_l is the lattice constant. The time t for the growth of fibrils of about $2 \mu\text{m}$ length is known from experiment and amounts to about 20 min.³ This corresponds to $n_{\text{MCS}} = 230\,000$ MCS for the simulation in Fig. 4(B). Since the jump probability for a free complex during each MCS is determined by $\exp(-E_s/kT)$, the waiting time τ is given by $\tau = (t/n_{\text{MCS}}) / \exp(-E_s/kT)$. For the simulation in Fig. 4 with $E_s = 3 \text{ kT}$, one obtains a diffusion coefficient of free FN-integrin complexes of $D = 7 \times 10^{-12} \text{ cm}^2/\text{s}$. This value is in satisfactory agreement with reported diffusion coefficients of α_5 integrins of adherent cells of $10^{-11} - 10^{-12} \text{ cm}^2/\text{s}$.¹⁸

It is worth noting that the characteristic features of the morphological diagram in Fig. 6 did not change significantly by varying E_i from 1–3 kT and n_{stretch} from 2 to 6. A somewhat higher growth rate of fibrils was found for larger values E_i due to a longer stay time of complexes at the focal adhesion. As a consequence, the transition of FN molecules into the stretched state occurs more frequently. Simulations on a doubled lattice with $N = 512$ did not show significant changes.

The proposed model of fibril formation is of course an approximation of the complex phenomenon. For example, the diffusion processes have been restricted to a 2D lattice. Actually, the FN fibrils are assembled in three dimensions. According to the SFM investigations in Ref. 7, the fibril height is about 20 nm. Nevertheless, integrin transport processes within the 2D cell membrane should play a major role in the overall rearrangement of FN molecules. Thus, the present 2D model seems to be an appropriate first approximation. Also, the squared shape of the focal adhesion might be considered as rather artificial. However, since the focal adhesions are connected to the actin cytoskeleton, the observed square lattice assembly of actin filaments²⁰ could cause a similar shape of the focal adhesion. On the other hand, tests in the simulations with a rounded shape of the focal adhesion did not hint to a significant shape dependence of fibril formation in the reported model.

Although FN and integrin do not form permanent links, both molecules were modeled together as one complex for the sake of simplicity. This approach is assumed to be reasonable because dissociation rate constants of FN-integrin bonds down to 0.012 s^{-1} have been determined experimentally.¹⁶ Hence, the lifetime of FN-integrin complexes is considerably longer than the mean waiting time between jumps of free complexes in the simulation of $\tau \approx 0.1 \text{ s}$. On the other hand, it is smaller than the total simulation time of about 1000 s. Thus, for a more accurate simulation of fibril formation, the present model has to be extended to also include the separate diffusion of FN and integrin molecules as well as binding and dissociation reac-

tions between them. To substantiate the predictions of the present theoretical study, further experimental investigations are desirable. The diffusion coefficients of integrins and FN molecules on the substrate could be measured by means of image correlation microscopy as demonstrated in Ref. 18. Furthermore, the interaction energy of FN with the substrate should be measured, for instance, by means of protein adsorption and exchange studies.⁸

IV. CONCLUSIONS

A phenomenological model was introduced to describe the development of characteristic nanometer scale features of FN fibrillogenesis by means of Monte Carlo simulations. As a main result, the simulations revealed the growth of paired FN nanofibrils in agreement with SFM observations in Ref. 7. The restriction of integrin transport to the 2D cell membrane, the myosin-driven transport of integrin-FN complexes along actin stress fibers, and a shielding effect during FN fibril assembly are proposed as main reasons for the paired nanofibril formation. The spacing between the nanofibrils of one fibril pair was controlled by the size of the focal adhesion when fibril growth starts. Besides paired nanofibrils also other typical growth patterns have been observed. A morphological diagram of these patterns has been established as a function of the FN-substrate and FN-FN interaction strengths. It shows branched FN clusters and tear-off of fibrils as characteristic patterns.

¹B. Alberts, D. Bray, J. Lewis, M. Raff, K. Roberts, and J. D. Watson, *Molecular Biology of the Cell*, 3rd ed. (Garland, New York, 1994), pp. 971–1000.

²B. Geiger, A. Bershadsky, R. Pankov, and K. M. Yamada, *Nat. Rev. Mol. Cell Biol.* **2**, 793 (2001).

³R. Pankov *et al.*, *J. Cell Biol.* **148**, 1075 (2000).

⁴V. Vogel, W. E. Thomas, W. W. Craig, A. Kramer, and G. Baneyx, *Trends Biotechnol.* **19**, 416 (2001).

⁵I. Wierzbicka-Patynowski and J. E. Schwarzbauer, *J. Cell. Sci.* **116**, 3269 (2003).

⁶T. Pompe, K. Keller, C. Mitdank, and C. Werner, *Eur. Biophys. J.* **34**, 1049 (2005).

⁷T. Pompe, L. Renner, and C. Werner, *Biophys. J.* **88**, 527 (2005).

⁸L. Renner, T. Pompe, K. Salchert, and C. Werner, *Langmuir* **20**, 2928 (2004).

⁹R. Bruinsma, *Biophys. J.* **89**, 87 (2005).

¹⁰T. Shemesh, B. Geiger, A. D. Bershadsky, and M. M. Kozlov, *Proc. Natl. Acad. Sci. U.S.A.* **102**, 12383 (2005).

¹¹A. Nicolas, B. Geiger, and S. A. Safran, *Proc. Natl. Acad. Sci. U.S.A.* **101**, 12520 (2004).

¹²A. Besser and S. A. Safran, *Biophys. J.* **90**, 3469 (2006).

¹³D. J. Irvine, A. Hue, A. M. Mayes, and L. G. Griffith, *Biophys. J.* **82**, 120 (2002).

¹⁴J. T. Finer, R. M. Simmons, and J. A. Spudich, *Nature (London)* **368**, 113 (1994).

¹⁵J. Howard, in *Physics of Bio-Molecules and Cells*, edited by H. Flyvbjerg, F. Jülicher, P. Ormos, and F. David (Springer, Berlin, 2002), Chap. 2, pp. 971–1000.

¹⁶F. Li, S. D. Redick, H. P. Erickson, and V. T. Moy, *Biophys. J.* **84**, 1252 (2003).

¹⁷T. Ohashi, D. P. Kiehart, and H. P. Erickson, *J. Cell. Sci.* **115**, 1221 (2002).

¹⁸P. W. Wiseman *et al.*, *J. Cell. Sci.* **117**, 5521 (2004).

¹⁹L. Renner, T. Pompe, K. Salchert, and C. Werner, *Langmuir* **21**, 4571 (2005).

²⁰O. Pelletier *et al.*, *Phys. Rev. Lett.* **91**, 148102 (2003).